Available online at www.sciencedirect.com
ScienceDirect
International Journal of Heat and Mass Transfer 51 (2008) 882–895
International Journal of HEAT and MASS TRANSFER
www.elsevier.com/locate/ijhmt

Error reduction, evaluation and correction for the intrusive optical four-sensor probe measurement in multi-dimensional two-phase flow

Xiuzhong Shen [a], Kaichiro Mishima [a,*], Hideo Nakamura [b]

[a] Research Reactor Institute, Kyoto University, Kumatori-cho, Sennan-gun, Osaka 590-0494, Japan
[b] Nuclear Safety Research Center, Japan Atomic Energy Agency, Tokai-mura, Ibaraki 319-1195, Japan

Received 23 May 2005

Abstract

The objective of the present study is to increase the reliability of multi-dimensional two-phase flow measurement using an intrusive optical four-sensor probe. We investigated the error reducing ways in fabricating an optical conical four-sensor probe from its basic principles and sought for a control technique to sharpen the optical fiber tip and a sensor assembling method for a four-sensor probe. According to the measuring process by a multi-sensor probe, measurement errors were classified into signal processing errors and hydrodynamic errors. The signal processing errors in the void fraction due to the threshold setting and those in the interfacial area concentration (IAC) due to the interface-pairing scheme and the threshold setting were analyzed and concluded to be tiny and negligible in the measurement by an optical four-sensor probe. The hydrodynamic errors were classified into oncoming bubble errors, receding bubble errors and transversal or missing bubble errors according to the bubble motion relative to the probe. The maximum errors in both IAC and void fraction due to oncoming bubbles in a four-sensor probe measurement were estimated to be 10%. The maximum underestimation for IAC in the traditional transversal bubble recovering way of a four-sensor probe was reported up to 30% when the intensity of bubble velocity fluctuation equaled to 1 and the bubble size was close to the probe separations between sensor tips. The maximum measurement errors in IAC and void fraction for the receding bubbles were valued at 31% and 38%, respectively, at low liquid and high gas flow rates conditions by performing evaluation experiments using downward-facing and upward-facing probes. To overcome the unsatisfactory measurement errors for the receding and transversal bubbles, we proposed expressions for the correction of IAC and void fraction in the four-sensor probe measurement in a multi-dimensional two-phase flow by adding the contribution of escaped bubbles due to the hindrance of the probe rear parts and that of transversal bubbles due to the existence of finite distance separation between the sensor tips.

Keywords: Multi-dimensional two-phase flow; Four-sensor probe; Interfacial area concentration; Void fraction; Error reduction, evaluation and correction

1. Introduction

Local measurements are of primary importance in knowing the characteristics of two-phase flows. Due to the success in pioneering work of Neal and Bankoff [1] and Miller and Mitchie [2] on conductivity and optical fiber probes, respectively, the phase discrimination probe has been widely utilized in two-phase flow studies as a local measuring device.

The interfacial area concentration (IAC) is defined as the interfacial area existing in a unit volume of the mixture and specifies the geometric capability of interfacial transfer. The principle of IAC measurement with a double- or four-sensor probe was proposed originally by Kataoka et al. [3]. Hibiki et al. [4] improved the double-sensor probe method by assuming the probability density function (PDF) of the angle between the interfacial velocity vector and the mean flow direction vector in a quadratic function form of the

* Corresponding author. Tel.: +81 72 451 2449; fax: +81 72 451 2637.
E-mail address: mishima@rri.kyoto-u.ac.jp (K. Mishima).

0017-9310/$ - see front matter © 2007 Elsevier Ltd. All rights reserved.
doi:10.1016/j.ijheatmasstransfer.2006.01.054

Nomenclature

A	determinant
A_0	basic determinant of a four-sensor probe
a	time-averaged interfacial area concentration (IAC), 1/m
D	pipe inner diameter, m
D_0	fiber core diameter, m
D_b	bubble diameter, m
D_1	flat end diameter of the conical fiber tip, m
D_s	outer diameter of stainless steel pipe, m
f	bubble frequency, 1/s
H_{max}	intensity of bubble velocity fluctuation
I_i	intensity of the incident ray, b/s
I_r	intensity of the reflection ray, b/s
I_{tr}	transmitted ray intensity, b/s
j	superficial velocity, m/s
l	minimum distance between the centers of two rear sensor fibers, m
N	interface number
n	refractive index
R	reflection coefficients or inner radius of a pipe, m
r	bubble or interface ratio or radial distance, m
$\mathbf{s}$	distance vector between two sensor tips, m
s_r	radial distance between two sensor tips, m
s_z	axial length between two sensor tips, m
$\mathbf{V}_i$	interfacial velocity vector, m/s
$\mathbf{V}_m$	measurable velocity vector between different sensor tips, m/s
V_{th}	threshold voltage, V
z	axial distance, m

Greek symbols

α	time-averaged void fraction
$\langle\alpha\rangle$	area-averaged void fraction
β	sensor tip half angle, °
Δt	time difference, s
η	angle between the distance vector of two sensor tips and the axis, °
Ω	time interval for averaging, s

Subscripts

0	front sensor of a multi-sensor probe
1, 2, 3	the 1th, 2th and 3th rear sensor of a multi-sensor probe
a, b, c	the ath, bth and cth figure in Fig. 1
b	the bth bubble
c	optical fiber cladding
co	optical fiber core
DFP	downward-facing probe
down	downward-moving bubbles
eff	effective bubbles or interfaces
esc	escaped bubbles
f	liquid phase
g	gas phase
k	the kth rear sensor of a multi-sensor probe, $k = 1, 2, 3$
l	the lth interface
rec	receding bubbles relative to a probe
t	total
tran	transversal bubbles
true	true value
UFP	upward-facing probe
up	upward-moving bubbles
x, y, z	x, y, and z axes

angle instead of the constant PDF postulated by Kataoka et al. [3]. The improved double-sensor probe method can measure the IAC effectively in a one-dimensional two-phase flow. However, when it is applied to the measurement in a multi-dimensional two-phase flow, the improved method will become unreliable due to its two main assumptions: (1) the interfacial velocity can be approximated by using the ratio of two sensor tip separation and time difference when the interface passing the two sensor tips and (2) the bubble is spherical in shape. On the other hand, the four-sensor probe methodology [3,5] gives an accurate measurement of IAC in principle without imposing the assumption of the spherical bubble shape and one-dimensional motion of bubbles. The original four-sensor probe method [3] enabled effective measurements of the IAC in a one-dimensional two-phase flow [6,7], but it did not tell how to deal with receding interfaces (namely interfaces that touch the rear sensor tip(s) ahead of the front sensor tip) in a multi-dimensional two-phase flow measurement. To apply the four-sensor probe method to a multi-dimensional two-phase flow measurement, Shen et al. [5] derived the interfacial measurement theorem relating the local instantaneous interfacial velocity to local measurable velocities based on the vector triangle analysis and improved the four-sensor probe method. Using the improved four-sensor probe method, not only oncoming interfaces (namely interfaces that touch the front sensor tip ahead of all rear sensor tips) but also receding ones could be measurable.

It should be mentioned here that the following four assumptions were employed in the derivation of the four-sensor probe method on the interfacial shape and velocity during the interface-sensor touching process and probe size: (1) the effect of interfacial curvature is neglected by assuming that the interface is a continuous and non-deforming curved surface, (2) the orientation of the normal vector at a fixed point in the continuous and non-deforming curved

surface is constant, (3) the velocity of the interface is constant and (4) the four-sensor probe is small in size relative to bubbles. Since it is inevitable that the intrusiveness and the finite size of the four-sensor probe and the difference between the assumed and real interfaces around the probe, it is very important to reduce, evaluate and correct the errors in the practical applications.

2. Principle of the measurement and four-sensor probe method

To effectively reduce, evaluate and correct the errors in the measurement of a multi-dimensional two-phase flow by the optical four-sensor probe method, it is necessary to review the principle of the measurement by the optical four-sensor probe method once again. It is of no doubt that the measurement errors are closely linked with the original principle and method.

2.1. Principle of the measurement by an optical probe

The working principle of an optical probe is based on the refraction and reflection laws in the optical fiber. A liquid–gas interface passing by the tip of the probe causes the laser system to change from one reflection state to another. Fig. 1 illustrates the measuring principle of a flat end optical probe. Referring to I_i and I_r as the intensities of the incident and reflected rays, respectively, and neglecting the absorption in the liquid and the gas phases, we can obtain the following equations for the total intensities of reflected ray for Fig. 1a–c, respectively

$$I_{ra} = I_{rl} + I_{ri} = I_i - I_{tra}, \tag{1}$$

$$I_{rb} = I_{rg} + I_{ri} = I_i - I_{trb}, \tag{2}$$

$$I_{rc} = I_{rl} = I_i - I_{trc}, \tag{3}$$

where I_{rl} and I_{rg} stand for the intensities of the reflected ray from the surface of the optical fiber tip contacting the liquid phase and the gas phase, respectively; I_{ri} is the intensity of the reflected ray from the interface of the two phases; I_{tr} is the intensity of the transmitted ray due to the refraction at the surface of the fiber tip; and the subscripts a, b and c denote the cases of a–c in Fig. 1, respectively. The contribution of I_{ri} causes a proximity detection that may induce an erroneous phase detection before the interface contacts the probe. Since the incident rays are not always parallel to the fiber axis and the actual interfaces are highly distorted, the I_{ri} from the interface of the two phases is negligible relative to the reflected ray from the surface of the optical fiber tip. Thus, we can obtain the following relation from Eqs. (1)–(3)

$$I_{ra} = I_{rc} \neq I_{rb}. \tag{4}$$

If we rearrange Eq. (4) in terms of the reflection coefficient, R, representing the fraction of the reflected ray to the incident ray intensities, we can obtain

$$R_a = R_c \neq R_b, \tag{5}$$

where $R_a = I_{ra}/I_i$, $R_b = I_{rb}/I_i$ and $R_c = I_{rc}/I_i$. For an unpolarized light, the reflection coefficient, R, is equal to unity when the total reflection occurs, otherwise it is equal to half the sum of the reflection coefficients for an electric field parallel and perpendicular, respectively, to the incidence plane [8]. Neglecting the difference between the incident angle in the fiber core and the refractive angle in the external medium with respect to the local normal at the fiber end boundary and rewriting these coefficients, we can obtain the reflection coefficients, R_a, R_b and R_c, for the three cases in Fig. 1, which are expressed by

$$R_a = R_c = \left(\frac{n_{co} - n_f}{n_{co} + n_f}\right)^2, \tag{6}$$

$$R_b = \left(\frac{n_{co} - n_g}{n_{co} + n_g}\right)^2, \tag{7}$$

where n_{co}, n_f and n_g stand for the refractive indexes for the fiber core, the liquid and the gas phases, respectively.

For a silica fiber with the core refractive index n_{co} of 1.46, the reflection coefficients for water phase ($n_f = 1.33$) and air phase ($n_g = 1.00$) were calculated as $R_a = R_c =$

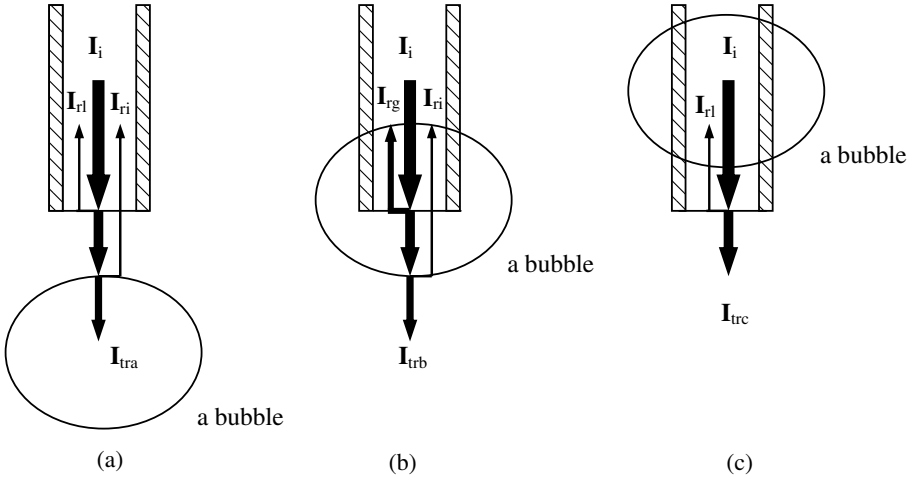

Fig. 1. Measuring principle of an optical probe.

0.00217 and $R_b = 0.0350$, respectively. The difference in the reflected fractions of the incident ray intensity in water and air will enable the detector to distinguish the existence of liquid or gas around the optical fiber tip.

An optical probe based on the above-mentioned principle can be used to detect the interface of two phases with different refractive indexes, such as that of water and steam, of water and air, of Freon and Freon-vapor and so on.

2.2. Four-sensor probe method

A four-sensor probe consists of a front sensor and three rear sensors. An interface can touch any sensor tip ahead of the others and leave behind the time when it touches any sensor tip. Among the interfaces which were detected by the main sensor tip (usually the front sensor tip) of a four-sensor probe, we can classify the interfaces into two groups, the effective interfaces and the missing interfaces. The effective interfaces are those which touch the front sensor tip and all of the three rear sensor tips. On the other hand, the missing interfaces are those which touch the front sensor tip but miss at least one of the three rear sensor tips.

According to the interfacial measurement theorem relating the local instantaneous interfacial velocity to local measurable velocities, Shen et al. [5] reported that the time-averaged local IAC from all of the oncoming and receding effective interfaces could be measured with the following equation, together with their new signal processing scheme to distinguish the same interface signal among the signals from different sensors of a four-sensor probe

$$a_{\text{eff}} = \frac{1}{\Omega}\sum_{l=1}^{N_{\text{eff}}} \frac{\sqrt{A_{01l}^2 + A_{02l}^2 + A_{03l}^2}}{|A_0|}, \tag{8}$$

where Ω, l, and N_{eff} denote the time interval for averaging, the lth effective interface, the number of effective interface within the time interval Ω, respectively; A_{01l}, A_{02l} and A_{03l} are directional determinants and A_0 the basic determinant. These determinants are expressed by

$$A_{01l} = \begin{vmatrix} \frac{1}{|\mathbf{V}_{m01l}|} & \cos\eta_{y01} & \cos\eta_{z01} \\ \frac{1}{|\mathbf{V}_{m02l}|} & \cos\eta_{y02} & \cos\eta_{z02} \\ \frac{1}{|\mathbf{V}_{m03l}|} & \cos\eta_{y03} & \cos\eta_{z03} \end{vmatrix}, \tag{9}$$

$$A_{02l} = \begin{vmatrix} \cos\eta_{x01} & \frac{1}{|\mathbf{V}_{m01l}|} & \cos\eta_{z01} \\ \cos\eta_{x02} & \frac{1}{|\mathbf{V}_{m02l}|} & \cos\eta_{z02} \\ \cos\eta_{x03} & \frac{1}{|\mathbf{V}_{m03l}|} & \cos\eta_{z03} \end{vmatrix}, \tag{10}$$

$$A_{03l} = \begin{vmatrix} \cos\eta_{x01} & \cos\eta_{y01} & \frac{1}{|\mathbf{V}_{m01l}|} \\ \cos\eta_{x02} & \cos\eta_{y02} & \frac{1}{|\mathbf{V}_{m02l}|} \\ \cos\eta_{x03} & \cos\eta_{y03} & \frac{1}{|\mathbf{V}_{m03l}|} \end{vmatrix}, \tag{11}$$

$$A_0 = \begin{vmatrix} \cos\eta_{x01} & \cos\eta_{y01} & \cos\eta_{z01} \\ \cos\eta_{x02} & \cos\eta_{y02} & \cos\eta_{z02} \\ \cos\eta_{x03} & \cos\eta_{y03} & \cos\eta_{z03} \end{vmatrix}, \tag{12}$$

where η_{x0k}, η_{y0k} and η_{z0k} $(0 \leqslant \eta_{x0k}, \eta_{y0k}, \eta_{z0k} \leqslant \pi)$ are the angles between the distance vector, $\mathbf{s}_{0k}$, $(\mathbf{s}_{0k} = |\mathbf{s}_{0k}|(\cos\eta_{x0k}\mathbf{i} + \cos\eta_{y0k}\,\mathbf{j} + \cos\eta_{z0k}\mathbf{k}))$ from front sensor tip 0 to rear one k, $(k = 1, 2, 3)$, and x, y and z axes, respectively; $\mathbf{V}_{m0kl}$ stand for the measurable velocities from front sensor tip 0 to rear one k, $(k = 1, 2, 3)$, for the lth interface, i.e.

$$\mathbf{V}_{m0kl} = \frac{\mathbf{s}_{0k}}{\Delta t_{0kl}}, \quad k = 1, 2, 3, \tag{13}$$

where Δt_{0kl} is the time when the lth interface immigrates from front sensor tip 0 to rear one k, $(k = 1, 2, 3)$. The orthogonal coordinate system is established with its apex at the front sensor tip of a four-sensor probe shown in Fig. 4a.

It should be mentioned here that Eq. (8) was first obtained by Kataoka et al. [3] in 1986 and Revankar and Ishii [6] also derived it in 1993. They calculated the local IAC of oncoming effective interfaces with this equation and dealt with receding effective interfaces as missing bubbles.

We shall discuss the measurement error evaluation and correction for the missing bubbles in Section 4.2.3.

3. Investigation tools

To conduct a local four-sensor probe measurement in a two-phase flow, it is essential to reproducibly manufacture desired four-sensor probes as a investigation tool. Since tapering the fine optical fiber tips to a point and reducing the cross-sectional measurement area of the probe can effectively minimize not only the number of escaped and missing bubbles but also the deformation of passing bubble interfaces, they are important ways in minimizing the measurement error to make a small and fine four-sensor probe. On the other hand, one should be aware that fine probe tips are vulnerable to flow induced vibrations which may cause additional measurement errors. In the present study, we tested the probes against a forced air flow and found that the flow induced vibrations may not be significant because of the stiffness of the optical fiber and the short length of the probe tips. So our attention should be focused on finding a way to fabricate a small and fine investigation tool.

The manufacturing process of the optical four-sensor probes consists of two key techniques, the fiber tip control and the sensor assembly for a four-sensor probe. The former is to sharpen the fiber tip to obtain a conical tip with a high reflection coefficient and the latter is to reduce the cross-sectional measurement area of the probe and to adjust the separation between sensor tips to a required distance.

3.1. Fiber tip control

The shape of a fiber tip (shown in Fig. 2) can be expressed by two parameters, namely the tip half angle β and the ratio of the tip flat end diameter D_1 to the fiber core

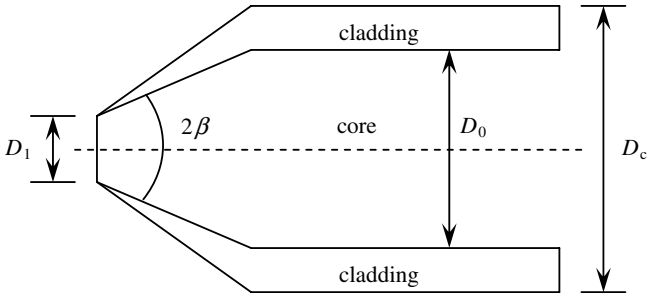

Fig. 2. Geometrical parameters for a fiber tip.

diameter D_0 (D_1/D_0) if the surface defect and cleanliness can be ignored. In practical cases, $0 < \beta \leqslant \pi/2$ and $0 < D_1/D_0 \leqslant 1$. When D_1/D_0 equals to 1 or the tip half angle β equals to $\pi/2$, the tip is flat or cleaved. When D_1/D_0 is 0 and β is smaller than $\pi/2$, the tip is conical. Considering the limitation of practical fiber tip manufacture, it is impossible to obtain a pure conical tip.

To optimize the optical probe geometry to improve its reflection coefficient, Cartellier and Barrau [9,10] changed the tip half angle β and the tip flat end diameter D_1 and studied their effects on the probe response by using a simplified optical simulations and well-controlled piercing experiments. According to their study, a probe tip with any combination of β and D_1/D_0 could be used for phase discrimination and the best sensitivity for detecting the presence of air or water was obtained when the tip half angle β was in the range of 40–50°. It should be mentioned here, however, that a small tip half angle β is preferable to reduce hydrodynamic errors around the fiber tip. Their investigation also revealed that a probe with flat tips or cleaved conical tips is more favorable for phase detection than a pure conical probe, due to its larger difference in the signal levels between the liquid and the gas.

Now we shall discuss the fiber tip processing techniques here. A flat fiber tip shape was formed by breaking off the fiber at which a small broken slot was ruptured firstly by a cutter. A conical fiber tip shape was obtained by using a popular melting and stretching technique. Cartellier and Barrau [9] reported that the reproducibility of this melting and stretching technique was satisfactory if an industrial micro-pipette puller was used. A conical fiber tip could be fabricated also by using the simple and traditional melting and stretching way, in which capillary forces are utilized to shape the extremity into a hemisphere after one's pull-cutting an optical fiber locally heated by a thin flame from a gas burner or a laser. Although the simple production method relies on personal skill, it is not very difficult for a beginner to make a good conical shape after several times of practice. An example of typical flat and conical tip ends of optical fibers with 125 μm in clad diameter (D_c) and 50 μm in core diameter (D_0) are illustrated in Fig. 3. The tip end diameters (D_1) are as small as 125 and 15 μm for the flat and conical fiber tip ends, respectively. The half angle (β) of the conical fiber tip end is about 8°.

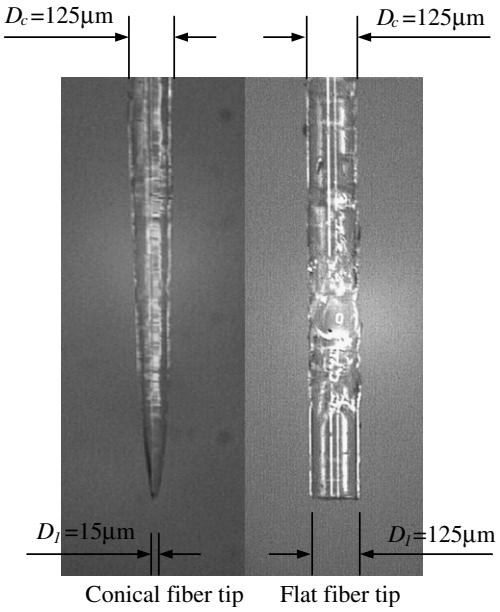

Fig. 3. Fiber tip shapes.

Cartellier and Barrau [9] also recommended an etching technique in making a conical fiber tip. This technique uses a chemical attack to eliminate the cladding and to form a conical tip, and the tip geometry can be accurately controlled by adjusting the attack time. The production also relies essentially on personal skill and the signal performance is lower due to the existence of the unclad fiber tip. Polishing may be a potential technique to overcome the deficiency, but it is quite delicate when applied to a tip size as small as a few tens of micrometers.

3.2. Sensor assembly for a four-sensor probe

In view of that the four-sensor probe has one front common sensor and three rear independent sensors, three pairs of double sensor probes, which could be accommodated to the small bubbles and the partly touching bubbles, can be formed in the measurement. Therefore, three measurable interfacial velocities $\mathbf{V}_{m0kl}$ from the front sensor tip, 0, to one of the three rear sensor tips, k, ($k = 1, 2, 3$), can be obtained at the front sensor tip point by measuring the separation distances and the time differences between the signals from three pairs of double sensor probes. The IAC measurement theory requires that the distance vectors, $\mathbf{s}_{0k}$, between the front sensor tip, 0, and rear sensor tips, k, ($k = 1, 2, 3$), are independent of each other, which implies that the basic determinant, $|A_0|$, should satisfy

$$A_0 = \begin{vmatrix} \cos\eta_{x01} & \cos\eta_{y01} & \cos\eta_{z01} \\ \cos\eta_{x02} & \cos\eta_{y02} & \cos\eta_{z02} \\ \cos\eta_{x03} & \cos\eta_{y03} & \cos\eta_{z03} \end{vmatrix} \neq 0. \tag{14}$$

Revankar and Ishii [6] arranged the locations of four conductivity sensors such that the tips of the sensors make an orthogonal coordinate system with the front sensor in

the apex and three rear sensors at the rear plane perpendicular to the flow direction. It is one of the arrangement examples of four sensors that meets the requirement of Eq. (14).

Under the spacing requirement of Eq. (14), we designed a new style of the optical four-sensor probe (shown in Fig. 4) by using a fiber with 125 μm in clad diameter (D_c) and 50 μm in core diameter (D_0). The supporting stainless steel pipes, with 0.35 mm in outer diameter (D_s), 0.09 mm in thickness and 40 mm in length, were arranged in a hexagon in a module shown in Fig. 4b. The four-sensor probe was made by threading the fibers with required tip shapes through the supporting pipes. An example of a fabricated conical optical four-sensor probe is illustrated in Fig. 4c and its geometrical specifications were listed in Table 1 by comparing to the active miniaturized four-sensor conductivity probe by Ishii and Kim [11]. The comparison shows that the present optical four-sensor probes are smaller than the active miniaturized four-sensor conductivity probe in the cross-sectional measurement area (which locates in a plane perpendicular to the z axis) and the distances between the front sensor tip and rear sensor ones. The decreases in the cross-sectional measurement area and the sensor tip distances will increase a probe's interfacial resolution and reduce its hydrodynamic error. The present optical four-sensor probe can measure the bubbles with the diameter ranging from 0.61 mm to slug bubbles.

4. Measurement errors and their evaluation

Although an ingenious design and fabrication of the optical four-sensor probe can greatly reduce the measurement errors, the errors still inevitably exist in the actual measurement. Here we shall find the way to evaluate and

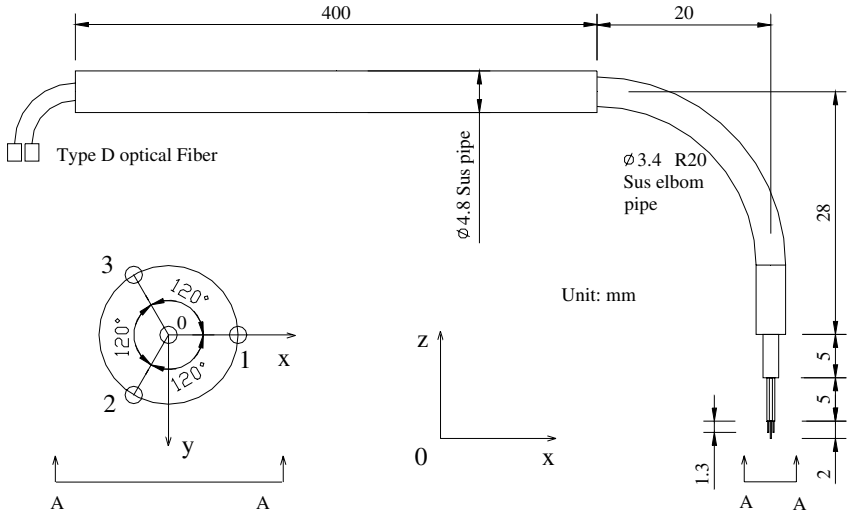

(a) Full view of a four-sensor probe

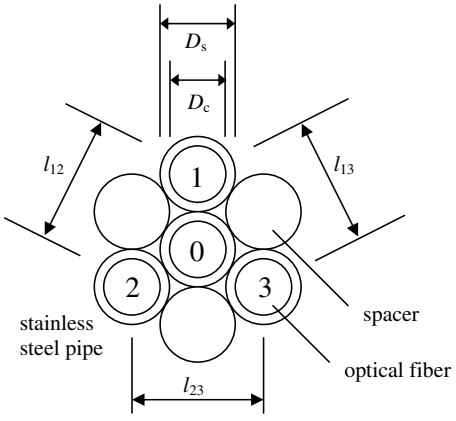

(b) A hexagon module

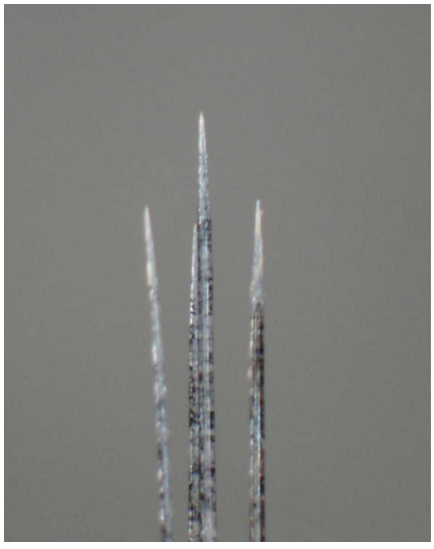

(c) Photo

Fig. 4. Design of typical optical four-sensor probe.

Table 1
Geometrical specifications of two four-sensor probes (unit: mm)

Typical probe	Max. D_c	$\|\mathbf{s}_{01}\|$	$\|\mathbf{s}_{02}\|$	$\|\mathbf{s}_{03}\|$	l_{12}	l_{13}	l_{23}	Cross-sectional measurement area
Optical	0.125	0.889	0.908	0.915	0.606	0.606	0.606	0.159
Conductivity	0.1	2.4	2.4	2.6	0.7	0.7	0.7	0.2

to correct the measurement errors. Some advances have been made in this field [12], but they were not completely known and corrected in the measurement. To estimate the errors, it is necessary to analyze and classify the measurement errors. According to the measuring process by a multi-sensor probe, we can classify measurement errors into signal processing and hydrodynamic errors, which will be discussed in the following sections.

4.1. Signal processing errors and their evaluation

Signal processing produces different errors for different parameters, such as void fraction and IAC, due to their different requirement for time differences obtained by the sensors in a probe. The void fraction requires the bubble residence time, Δt_{0b}, for the bth bubble, while the IAC needs the time difference, Δt_{01l}, when the lth interface passes through two neighboring sensor tips, 0 and 1 (see Fig. 5). Consequently, we know that the signal processing error for void fraction may considerably decrease if the sensor response time, namely, the rising or falling time at the phase transition, could be shortened and that the signal processing error for IAC is mainly linked with the right selection of the output signals from different sensors for the same interface.

The response time usually originates from two sources: (1) the measurement system (such as sensor tip shape, laser transmission and electrical circuitry) and (2) the sensor tip intrusion (interfacial deformation in a bubble, liquid film drainage around the sensor tip, etc.). The resulting slopes in the raw signals during the response time may bring about some difficulties in selecting an appropriate threshold, V_{th}, to discriminate the gas and the liquid phases in signal processing. If different thresholds, V_{th}, and $V_{th,1}$, were selected as illustrated in Fig. 5, different bubble residence times, Δt_{0b} and $\Delta t_{0b,1}$ would be obtained in the signal processing. Hence it is impossible to avoid this signal processing error in void fraction measurement using an optical or conductivity probe. However, the response time of an optical or conductivity probe is much shorter and is almost negligible compared to the bubble residence time, especially in the case of an optical probe, in which the response time is even much smaller than that of a conductivity probe.

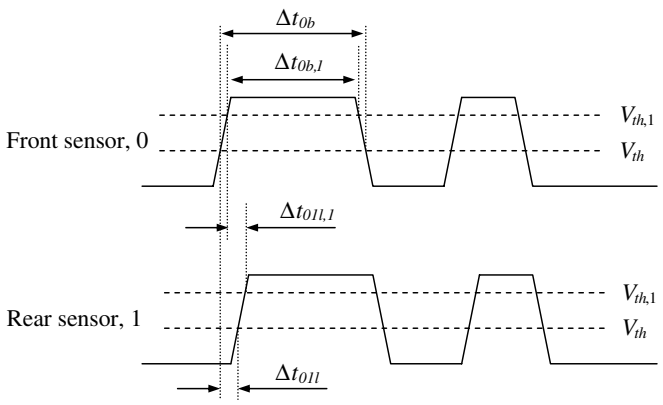

Fig. 5. Processing of two sensor raw signals.

When the lth interface touches or leaves the different sensor tips, 0 and 1, the output rising or falling signal of the sensor 0 is similar to that of the sensor 1. Thus we know that the time difference, Δt_{01l}, at threshold, V_{th}, was very close to the time difference, $\Delta t_{01l,1}$, at different threshold, $V_{th,1}$ and the signal processing error relating to the response time in the IAC measurement was not so significant as that in void fraction measurement. As a result of that, the signal processing errors due to the response time are tiny and negligible in both the void fraction and IAC measurement with an optical probe. This point is further confirmed in practical optical four-sensor probe measurements, in which the reduction in the void fraction was estimated to be 1.05% and the IAC measured with the interface-pairing signal processing scheme of Shen et al. [5] to be 0.156% when the signal threshold was increased by 20%.

It is essential to select the right interface signal from the outputs of different sensors of a multi-sensor probe in the IAC measurement because the sequential signals detected by different sensors are not always corresponding to the same interface and the residence time in the same gas or liquid phase are not exactly the same for different sensors. By assuming a forward motion of bubbles relative to a fixed probe, Revankar & Ishii [6,13] proposed a bubble-pairing signal processing scheme to discriminate a right pair of signals out of those detected by different sensors. Usually we define bubbles which touch the front sensor tip and miss one or more than one rear sensor tip(s) in a probe as the missing bubbles. But according the bubble-pairing signal processing scheme, bubbles which touch the front sensor but do not meet the requirements of their scheme are designated as missing bubbles, regardless of their touching all of the four-sensor tips. Hence all receding bubbles relative to the probe and all bubbles with a longer residence time in one or more rear sensor tip(s) than that in the front sensor tip are treated as missing bubbles. The contribution of each missing bubble for IAC is estimated by the average value of IAC of all effective bubbles. This treatment may definitely cause a certain amount of signal processing error in the IAC measurement. Le Corre and Ishii

[12] reported in their numerical experiments that an underestimation up to 30% was observed in this conventional IAC recovering way for the missing bubbles. When transversal and receding bubble motions prevail, this signal processing scheme is not effective because of the extremely low fraction of effective bubbles, resulting in a large signal processing error.

To meet the need for IAC measurement in a multi-dimensional bubbly flow, Shen et al. [5] proposed an interface-pairing signal processing scheme to pick up a pair of signals for an identical interface detected by different sensors of a multi-sensor probe. In this scheme, according to the time sequencing each interfacial signal from the front sensor is compared with a sequence of signals from each rear sensor to find out the corresponding interfacial signal. This signal processing scheme was verified by comparing the results with the observations of raw signals, which showed that all of the effective interfaces touching both front sensor and all rear sensors were counted based on this scheme. Thus the signal processing error linked with the right selection of the signals for identical interface from the outputs of different sensors was minimized to be 0 by the present signal processing scheme.

The above-mentioned discussion shows that the signal processing error in the void fraction measurement with an optical probe is small and that in IAC measurement using an optical four-sensor probe with the interface-pairing signal processing scheme of Shen et al. [5] can be ignored in a practical application.

4.2. Hydrodynamic errors and their evaluation

Hydrodynamic effects around an intrusive probe play the most important role in producing measurement errors and can make the measurement unreliable at an extremely low flow rate. It is, accordingly, necessary to evaluate the errors based on the bubble movements before the application of an intrusive probe to a two-phase flow.

According to the bubble movements relative to an intrusive probe in a multi-dimensional two-phase flow, bubbles can be divided into three groups, oncoming (on), receding (rec) and transversal (tran) bubbles, which were illustrated in Fig. 6a–c, respectively. Oncoming bubbles move against the probe and accordingly touch the front sensor tip first ahead of the rear sensor tips. Receding bubbles move along the probe sensors from the rear and accordingly touch the rear sensor tip(s) first ahead of the front sensor tip. Finally transversal bubbles move in a direction nearly perpendicular to the probe sensors, touch the front sensor tip, but miss the rear sensor tip(s) and are usually called missing bubbles. For a downward-facing intrusive probe in an upward two-phase flow, upward-moving bubbles are oncoming ones and downward-moving bubbles are receding ones.

When upward-moving bubbles are dominant and downward-moving bubbles negligible at high j_f and low j_g conditions in an upward two-phase flow, the flow can be simplified as one-dimensional. On the other hand, when upward-moving bubbles decrease and downward-moving bubbles become remarkable at low j_f and high j_g conditions, the flow shows its multi-dimensional nature [14].

To know the constituent ratios of upward-moving, downward-moving and transversal bubbles in a upward bubbly two-phase flow, we performed an experiment in a vertical pipe with 0.2 m inner diameter (D). The investigation experiment were made at the height-to-diameter ratio of 113 (namely, $z/D = 113$) in the pipe by using a downward-facing optical double-sensor probe of 0.460 mm in its separation. Referring to f_t as the bubble frequency detected by the front sensor of a double-sensor probe, f_{up} as the bubble frequency whose bubbles move upwardly and touch the front sensor tip ahead of the rear sensor tip, f_{down} as the bubble frequency whose bubbles move downwardly and touch the rear sensor tip ahead of the front sensor tip, and f_{tran} as the bubble frequency whose bubbles move nearly horizontally and touch the front sensor tip but miss the rear sensor tip, the ratios of f_{up}/f_t, f_{down}/f_t and f_{tran}/f_t stand for the upward-moving bubble or interface ratio (r_{up}), the downward-moving bubble or interface ratio (r_{down}) and transversal bubble or interface ratio (r_{tran}), respectively. The radial profiles of these ratios are shown in Fig. 7a and b for a low liquid flow rate ($j_f = 0.0350$ m/s) and a relatively high liquid flow rate ($j_f = 0.277$ m/s) conditions, respectively, and the corresponding flow patterns and the area-averaged void fraction $\langle\alpha\rangle$ are listed in Table 2. Comparing with the flow observation, we can get the following points from Fig. 7a and b: (1)

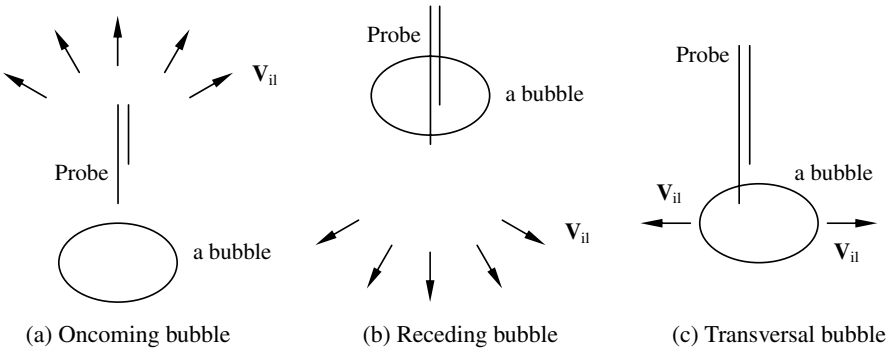

Fig. 6. Bubble relative movement analysis.

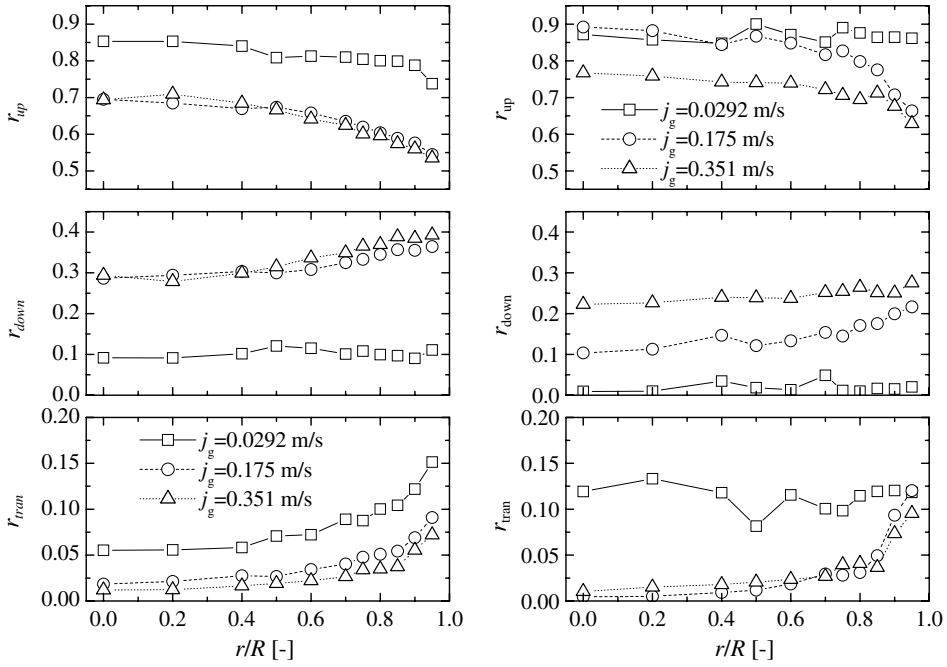

(a) Low liquid flow rate (j_f=0.0350m/s, z/D=113)

(b) Relative high liquid flow rate (j_f=0.277m/s, z/D=113)

Fig. 7. The radial profiles of r_{up}, r_{down} and r_{tran}.

Table 2
Flow patterns and area-averaged void fraction at various flow conditions

z/D	j_f (m/s)	j_g (m/s)	$\langle\alpha\rangle$	Flow patterns
113	0.0350	0.0292	0.0452	Agitated bubbly flow
		0.175	0.215	Churn slug
		0.351	0.283	Churn slug
	0.277	0.0292	0.0231	Undisturbed bubbly flow
		0.175	0.221	Churn bubbly
		0.351	0.240	Churn slug

Most of bubbles (over 65%) move upwardly even when an intensive secondary flow prevails. (2) Downward-moving bubbles are negligible (less than 5%) when a one-dimensional bubbly flow prevails in the flow path (see $j_f = 0.277$ m/s and $j_g = 0.0292$ m/s in Fig. 7b), however, in a multi-dimensional bubbly flow, downward-moving bubbles must be measured independently due to its large contribution. (3) The upward-moving bubble ratio increases with increasing j_f and decreasing j_g, and the downward-moving and transversal bubble ratios accordingly decrease with increasing j_f and decreasing j_g. (4) The upward-moving bubble ratios decreased in the radial direction, and the downward-moving and transversal bubble ratios accordingly increased in the radial direction. (5) At a low liquid flow rate and a high gas flow rate, the j_g increase cannot further increase the downward-moving bubble ratio significantly which shows that there exists a maximum downward-moving bubble ratio (nearly 38.8%) in the upward multi-dimensional two-phase flow. The cross-sectional area-averaged void fraction $\langle\alpha\rangle$ is about 0.283 when the maximum downward-moving bubble ratio happens near the wall of the pipe. (6) About 5% of the bubbles move transversally, although measured transversal bubble ratio might vary with the probe geometry and the local flow conditions.

4.2.1. Error evaluation for oncoming bubbles

Kim et al. [15] benchmarked the void fraction and IAC measurements of a four-sensor probe for upward-moving stable slug bubbles generated in a stagnant liquid test column at the flow conditions of $j_f = 0.321$ m/s and (1) $j_g = 0.052$ m/s, (2) $j_g = 0.179$ m/s and (3) $j_g = 0.432$ m/s by using image analysis. Their comparisons between the values obtained by the four-sensor probe and those calculated based on the image analysis showed that the agreements were within ±10%. It should be mentioned here that their benchmark experiments were arranged in a one-dimensional stable slug bubble flow region, that their results might verify the validation of void fraction and IAC measurements for the oncoming bubbles touching a four-sensor probe and that the void fraction and IAC measurements for receding bubbles touching a four-sensor probe should be validated in other specially designed experiments.

4.2.2. Error evaluation for receding bubbles

Due to the hindrance by the rear supporting part of an intrusive probe, receding bubbles are expected to be more remarkably disturbed than oncoming bubbles in the measurement. When the receding bubble ratio reaches a certain degree, the hydrodynamic errors generated from bubble

escape, interfacial deformation and bubble slowing down due to the hindrance by the probe rear part could be large enough to affect the reliability of void fraction and IAC measurements with the intrusive probe.

To have an insight into the origin of measurement uncertainty and to evaluate the measurement errors for oncoming and receding bubbles, we performed experiments for a one-dimensional upward two-phase flow in a vertical large diameter pipe of 0.2 m in inner diameter by using typical double-sensor probes. The probes were placed in two ways, downward-facing (DFP) or upward-facing (UFP) (shown in Fig. 8a and b), at the same height and the same flow conditions. These comparing measurements were made at three heights, $z/D = 41.5$, 82.8 and 113, under each flow condition. The flow pattern was undisturbed bubbly flow and the area-averaged void fraction $\langle\alpha\rangle$ ranged from 0.0133 to 0.0267 in these experiments. Fig. 9 illustrates the comparisons of the results for IAC, void fraction and bubble frequency measured by using the downward-facing and upward-facing probes in one-dimensional two-phase flow. The figures on the left and the right are for relatively high ($j_f = 0.277$ m/s, $j_g = 0.0389$ m/s) and low ($j_f = 0.0533$ m/s, $j_g = 0.0195$ m/s) flow rates, respectively, and the top, the middle and the bottom figures show the radial profiles of relative IAC (a_{UFP}/a_{DFP}), relative void fraction ($\alpha_{UFP}/\alpha_{DFP}$) and relative bubble frequency (f_{UFP}/f_{DFP}), respectively. The data points at $z/D = 41.5$, 82.8 and 113 are denoted by the open symbols of square, circle and triangle, respectively, in Fig. 9.

Since oncoming bubbles are dominant and the bubble hydrodynamic effect is considered to be negligible for the downward-facing double-sensor probe in a one-dimensional upward two-phase flow, the IAC (a_{DFP}), void fraction (α_{DFP}) and bubble frequency measured by the downward-facing probe should be close to the true values of IAC (a_{true}), void fraction (α_{true}) and bubble frequency. Thus, we have

$$a_{true} \approx a_{DFP}, \tag{15}$$

$$\alpha_{true} \approx \alpha_{DFP}. \tag{16}$$

On the other hand, receding bubbles are dominant for an upward-facing probe in a one-dimensional upward two-phase flow. From Fig. 9, we see that the upward-facing probe picked up only about 33% bubbles, 19% void fraction and 38% IAC and the rest bubbles, the rest void fraction and the rest IAC were lost because of hydrodynamic effects (namely, the bubble escape, interfacial deform and bubble slowing down effects) due to the hindrance of the upstream part of the upward-facing probe when the receding bubble ratio (r_{rec}), i.e., upward-moving bubble ratio, was around 83% (estimated from Fig. 7) in the upward bubbly two-phase flow. The measured relative bubble frequency was larger than the relative void fraction due to the fact that the bubbles detected by the upward-facing double-sensor probe were relatively small in size. The measured relative IAC value was greater than the relative bubble frequency and void fraction values, owing to the small bubble size and the bubble slowing down and the interfacial deformation effects near the upward-facing probe. The experimental result clearly indicates that the upstream part of the probe has a dominant effect on the receding bubbles, which cause a lot of receding bubbles to escape from the detection of the probe tip. The escaped bubbles were basically responsible for the large percentages of lost bubbles, lost void fraction and lost IAC. The IAC ratio (a_{esc}/a_{true}) and the void fraction ratio ($\alpha_{esc}/\alpha_{true}$) for escaped bubbles in the one-dimensional upward two-phase flow could be approximated by

$$a_{esc}/a_{true} \approx (a_{DFP} - a_{UFP})/a_{DFP}, \tag{17}$$

$$\alpha_{esc}/\alpha_{true} \approx (\alpha_{DFP} - \alpha_{UFP})/\alpha_{DFP}. \tag{18}$$

With this approximation, measured a_{esc}/a_{true} and $\alpha_{esc}/\alpha_{true}$ are plotted against the receding bubble ratio (r_{rec}) in

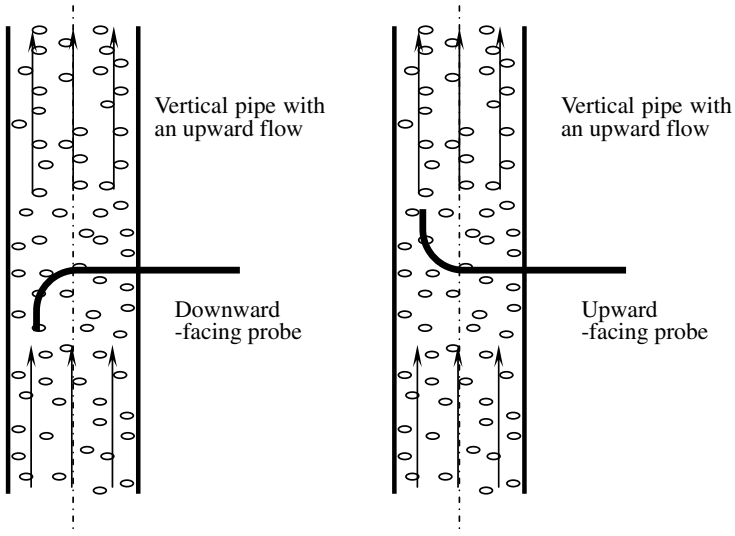

(a) Downward-facing probe (b) Upward-facing probe

Fig. 8. Downward-facing probe and upward-facing probe.

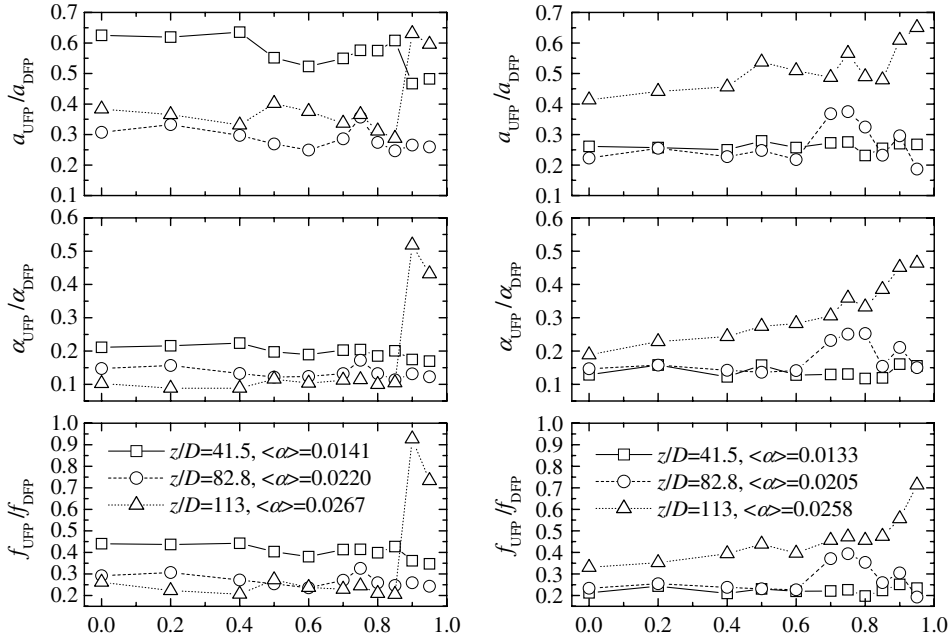

(a) j_f=0.277 m/s, j_g=0.0389 m/s (Undisturbed bubbly flow)

(b) j_f=0.0533 m/s, j_g=0.0195 m/s (Undisturbed bubbly flow)

Fig. 9. Result comparison between the downward-facing and upward-facing probes.

Fig. 10a and b, respectively. This figure shows that about 62% of IAC and 81% of void fraction are missed in the measurement due to the hindrance by the rear part of the upward-facing probe in the upward two-phase flow in which 83% of bubbles are receding bubbles with respect to the upward-facing probe. When the receding bubble ratio equals to zero, the lost IAC and void fraction attributed to the escaped bubbles due to the hindrance by the probe rear part should be zero too. Therefore, we can know that the a_{esc}/a_{true} and $\alpha_{esc}/\alpha_{true}$ due to the upstream intrusiveness of the probe rear part are closely linked with or mainly determined by the receding bubble ratio (r_{rec}) which depends on the local two-phase flow conditions. Le Corre and Ishii [12] performed one hundred simulations with random double-sensor probe geometry characteristics (s_r in the range from 0 mm to 300 μm and s_z from 1 to 3 mm), random bubble diameters (D_b in the range from 1 to 3 mm) and random bubble velocity fluctuation intensities (H_{max} in the range from 0 to 1) and concluded that the measurement error among all appreciable bubbles by the front sensor tip could expressed as a function of the missing bubble ratio only. Presumably, we are thinking that the receding bubble ratio (r_{rec}) may be the only dominating parameter to determine a_{esc}/a_{true} and $\alpha_{esc}/\alpha_{true}$ due to the upstream intrusiveness of the probe rear part in a measurement. Here, it should be mentioned that the receding bubble ratio (r_{rec}) determined by the local flow condition is an important parameter to signify the prevalence of bubble secondary flow in a downward-facing probe measurement in an upward two-phase flow and is easily calculated by the data processing software.

By fitting the experimental data with a polynomial function and considering the extreme case of $r_{rec} = 0$, we suggest the following linear functions to calculate a_{esc}/a_{true} and $\alpha_{esc}/\alpha_{true}$ from the receding bubble ratio, r_{rec},

$$a_{esc}/a_{true} = 0.8 r_{rec} \quad r_{rec} \in [0,1], \tag{19}$$

$$\alpha_{esc}/\alpha_{true} = 0.98 r_{rec} \quad r_{rec} \in [0,1]. \tag{20}$$

Eqs. (19) and (20) are illustrated, together with measured values of a_{esc}/a_{true} and $\alpha_{esc}/\alpha_{true}$, in Fig. 10a and b, respectively.

From the above two equations, we can predict that the lost IAC and the lost void fraction relating to the bubble escape effect due to the upstream existence of the intrusive probe rear part will reach 80% and 98% of the true values, respectively, when no oncoming bubble and no transversal bubble exist ($r_{rec} = 1$), and that the lost IAC and the lost void fraction are within 4% and 4.9% of the true values, respectively, in the downward-facing probe measurement in a one-dimensional upward two-phase flow since the receding bubble ratio is less than 5%. It is worth here referring to double-sensor probe benchmarking experiments of Kim et al. [16]. They compared the IAC obtained by a downward-facing double-sensor probe with that measured by image analysis in a one-dimensional upward air–water two-phase flow in a rectangular duct with the void fraction less than 5% and concluded that the relative percent difference between the two methods is within 10%. The comparison between the present prediction and the benchmarking experiment result of Kim et al. [16] revealed that they were

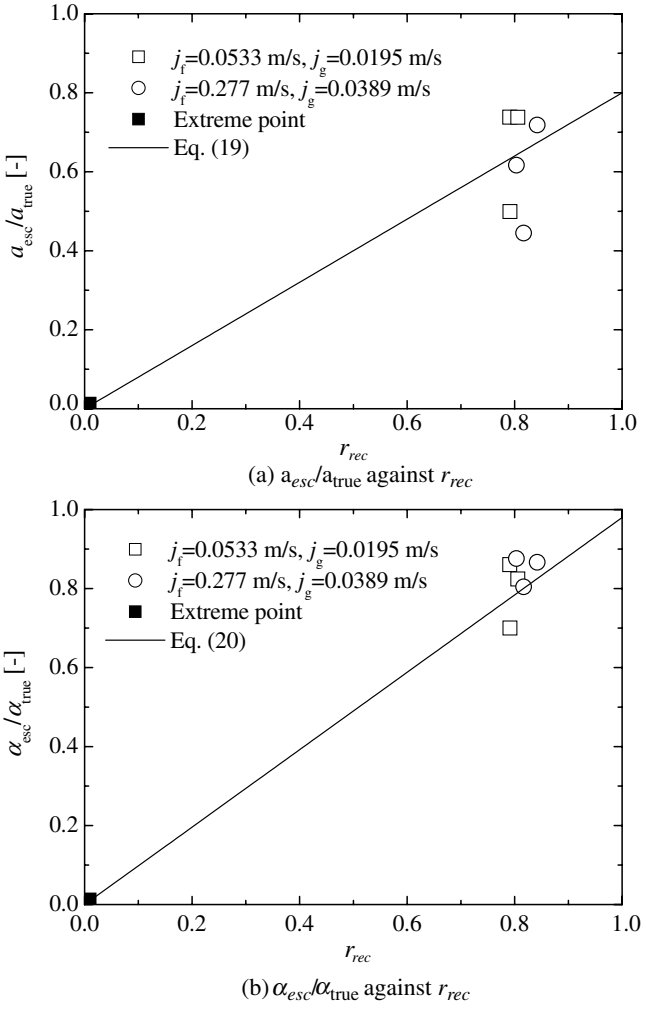

Fig. 10. a_{esc}/a_{true} and $\alpha_{esc}/\alpha_{true}$ against r_{rec}.

in accordance with each other if other measurement errors such as missing bubble error et al. were considered. Fig. 7 shows that the maximum downward-moving bubble ratio in the multi-dimensional two-phase flow in a vertical large diameter pipe, namely, the maximum receding bubble ratio relative to the downward-facing multi-sensor probe, happened at low liquid and high gas flow rates conditions and was estimated at about 38.8%. Thus we can know that the maximum lost IAC and lost void fraction due to the existence of probe rear part are 31% relative to the true IAC and 38% relative to the true void fraction, respectively, which occurs only at low liquid and high gas flow rates conditions.

4.2.3. Error evaluation and correction for transversal or missing bubbles

Due to the existence of the distance separation between the sensor tips, the transversal or missing bubbles usually touch the front sensor tip and miss at least one of the rear sensor tips in the multi-sensor probe measurement. In the classical procedure to deal with the missing bubbles in the one-dimensional bubbly flow, the missing bubbles were treated as if they possess the average measured interface velocity in the surface normal direction for the effective bubbles. Thus the true IAC, a_{true}, is approximated by multiplying the measured IAC from the effective bubbles, a_{eff}, by a correction term

$$a_{true} = \frac{N_t}{N_{eff}} a_{eff}, \tag{21}$$

where N_t and N_{eff} were the total interface number detected by the front sensor of a probe and the effective interface number sensed by all sensors of a probe. Wu and Ishii [17] and Le Corre and Ishii [12] found that the missing bubbles were underestimated in this IAC recovering method because the missing bubbles are generally the smallest bubbles or the bubbles caught on the edge. Le Corre and Ishii [12] also reported that an underestimation of this recovering method up to 30% was observed in their numerical study on a four-sensor probe when the intensity of bubble velocity fluctuation equaled to 1 and the bubble size was close to the probe separations between sensor tips. Based on a study on the effects of the probe geometry, bubble size and the intensity of the bubble velocity fluctuation to the IAC measurement, Wu and Ishii [17] gave a correction factor, which depended on the previous parameters, in the IAC measurement method with a double-sensor probe. However, Le Corre and Ishii [12] pointed out that the correction method of Wu and Ishii [17] had some difficulties in accurately measuring the bubble size and the intensity of the bubble velocity fluctuation and in reliably characterizing the flow with numerous parameters involved and that their correction method was based on an isotropic flow velocity field model, which was not reliable especially in the regions close to the wall. Therefore, Le Corre and Ishii [12] proposed a different correction procedure based on the missing bubble ratio, i.e., the transversal bubble ratio, r_{tran}, only by using numerical evaluation for the four-sensor probe measurement,

$$a_{true} = \frac{1}{\sqrt{1-\sqrt{2.4 r_{tran} - 1.5 r_{tran}^2}}} a_{eff} \quad r_{tran} \in [0, 0.7]. \tag{22}$$

Although they assumed that the bubbles were spherical in their study, they stated that their corrections could be applied to distorted bubble as well with a reasonable degree of accuracy in practical measurement.

5. A correction method for multi-dimensional two-phase flow measurement

The previous studies showed that the maximum IAC and void fraction measurement error from the perturbation due to the rear supporting part of a probe would reach 31% and 38% at low liquid and high gas flow rates conditions in the downward-facing probe measurement in an upward two-phase flow of large diameter pipe. There are three possible sources for these unsatisfactory measurement errors, (1) the interface deformation, (2) the change in interfacial velocity magnitude and direction, and (3) the bubble

escape. Since there exist the similarity in the interfacial deformation for different sensors in a multi-sensor probe and the similarity in the interfacial deformation for the bubble-touching and bubble-leaving processes of any sensor, the interface deformation effect will not greatly affect the measured time difference when an interface passes through the two different sensors and the measured residence time of a sensor in a bubble. The bubble deformation accordingly cannot be a large source of the IAC and void fraction measurement error. When a sensor pierces into a bubble, the bubble may slow down and deviate in the velocity direction. We note that, if the bubble has a much larger size than the sensor diameter, the counteracting force of the surface tension on a bubble surface is very weak and the interfacial velocity change and the measurement error from the sensor piercing will accordingly be tiny. Thus we can know that the above-mentioned unsatisfactory measurement errors are mainly from the bubble escape. If we only apply the probe to the two-phase flow, in which the bubbles are much larger than the probe size, the escaped bubbles among the oncoming bubbles will be negligible. The escaped bubbles among the receding bubbles are due to the upstream intrusiveness of the probe rear part and accordingly should be corrected in the practical measurement in its corresponding flow range. It is worthwhile to mention here that the hindrance by the whole rear part of an intrusive probe is much larger than that by the exposed fine and short fiber rear parts only. Therefore, the differences in the lost IAC and lost void fraction due to the existence of the probe rear part between double-sensor probe and four-sensor probe will be tiny.

In view of the correction for transversal bubbles done by Le Corre and Ishii [12] and the analysis for the lost IAC and lost void fraction due to the existence of the probe rear part, we proposed the following expressions to calculate the true IAC (a_{true}) and the true void fraction (α_{true}) for the downward-facing four-sensor probe measurement in an upward multi-dimensional two-phase flow,

$$a_{\text{true}} = \frac{1}{\sqrt{1-\sqrt{2.4r_{\text{tran}}-1.5r_{\text{tran}}^2}}} \times \frac{1}{1-0.8r_{\text{rec}}} a_{\text{eff}} \quad r_{\text{rec}} \in [0,1], \quad r_{\text{tran}} \in [0,0.7], \tag{23}$$

$$\alpha_{\text{true}} = \frac{1}{1-0.98r_{\text{rec}}} \alpha_{\text{eff}} \quad r_{\text{rec}} \in [0,1], \tag{24}$$

where a_{eff} can be computed by using Eq. (8) and α_{eff} can be obtained according to the detection of the front sensor tip, the r_{tran} and r_{rec} are the transversal or missing bubble ratio and receding bubble ratio, respectively.

6. Conclusions

How to reduce, evaluate and correct the measurement errors of a four-sensor probe are of great importance not only in improving the reliability of four-sensor probe, but also in establishing the research method for a multi-dimensional two-phase flow. In view of this, we discussed a reproducible way to make the optical four-sensor probe and recommended two key fabricating techniques, i.e., the fiber tip control and the sensor assembly, to reduce the measurement error, based on the basic principle analysis on an optical conical four-sensor probe.

To evaluate the measurement errors, we classified the measurement error into the signal processing error and the hydrodynamic error in a practical probe measurement and estimated the signal processing error to be tiny and negligible in the void fraction and IAC measurement by an optical multi-sensor probe (together with the interface-pairing signal processing scheme of Shen et al. [5]). According to the bubble movements relative to an intrusive probe, we further classified the bubbles in a two-phase flow into three groups, the oncoming, the receding and transversal bubbles, i.e., the upward-moving, downward-moving and transversal bubbles, in a downward-facing probe measurement in an upward two-phase flow. Their constituent ratios were experimentally investigated in the multi-dimensional upward two-phase flow of a vertical large diameter pipe. The maximum IAC measurement error for the oncoming bubbles was appraised at 10% based on the effort of Kim et al. [15]. The maximum IAC and void fraction measurement error for the receding bubbles was at 31% and 38%, respectively, by performing evaluation experiments using downward-facing and upward-facing probes. And the maximum IAC measurement error for the transversal bubbles was at 30% according to the numerical evaluation of Le Corre and Ishii [12].

With regard to the unsatisfactory measurement errors for the receding and transversal bubbles, we proposed a correction method for the four-sensor probe measurement in a multi-dimensional two-phase flow by adding the lost IAC and the lost void fraction linking with the escaped bubbles due to the existence of the probe rear parts for the receding bubbles and adopting the correction way of Le Corre and Ishii [12] for the transversal bubbles.

References

[1] L. Neal, S. Bankoff, A high resolution resistivity probe for determination of local properties in gas–liquid flow, AIChE J. 9 (4) (1963) 490–494.
[2] N. Miller, R. Mitchie, Measurement of local voidage in liquid/gas two-phase flow systems using an universal probe, J. Brit. Nucl. Energy Soc. 2 (1970) 94–100.
[3] I. Kataoka, M. Ishii, A. Serizawa, Local formulation and measurements of interfacial area concentration in two-phase flow, Int. J. Multiphase Flow 12 (4) (1986) 505–529.
[4] T. Hibiki, T. Hogsett, M. Ishii, Local measurement of interfacial area, interfacial velocity and turbulence in two-phase flow, Nucl. Eng. Des. 184 (2–3) (1998) 287–304.
[5] X. Shen, Y. Saito, K. Mishima, H. Nakamura, Methodological improvement of an intrusive four-sensor probe for the multi-dimensional two-phase flow measurement, Int. J. Multiphase Flow 31 (5) (2005) 593–617.
[6] S. Revankar, M. Ishii, Theory and measurement of local interfacial area using a four sensor probe in two-phase flow, Int. J. Heat Mass Transfer 36 (12) (1993) 2997–3007.

[7] X. Shen, Y. Saito, K. Mishima, H. Nakamura, A study on the characteristics of upward air–water two-phase flow in a large pipe, Exp. Therm. Fluid Sci. 31 (1) (2006) 21–36.
[8] T. Okoshi, Optical Fibers, Academic Press, London, 1982.
[9] A. Cartellier, E. Barrau, Monofiber optical probes for gas detection and gas velocity measurements: conical probe, Int. J. Multiphase Flow 24 (8) (1998) 1265–1294.
[10] A. Cartellier, E. Barrau, Monofiber optical probes for gas detection and gas velocity measurements: optimised sensing tips, Int. J. Multiphase Flow 24 (8) (1998) 1295–1315.
[11] M. Ishii, S. Kim, Micro four-sensor probe measurement of interfacial area transport for bubbly flow in round pipes, Nucl. Eng. Des. 205 (1–2) (2001) 123–131.
[12] J.-M. Le Corre, M. Ishii, Numerical evaluation and correction method for multi-sensor probe measurement techniques in two-phase bubbly flow, Nucl. Eng. Des. 216 (1–3) (2002) 221–238.
[13] S.T. Revankar, M. Ishii, Local interfacial area measurement in bubble flow, Int. J. Heat Mass Transfer 35 (4) (1992) 913–925.
[14] X. Shen, K. Mishima, H. Nakamura, Two-phase phase distribution in a vertical large diameter pipe, Int. J. Heat Mass Transfer 48 (1) (2005) 211–225.
[15] S. Kim, X.Y. Fu, X. Wang, M. Ishii, Study on interfacial structures in slug flows using a miniaturized four-sensor conductivity probe, Nucl. Eng. Des. 204 (1–3) (2001) 45–55.
[16] S. Kim, X.Y. Fu, X. Wang, M. Ishii, Development of the miniaturized four-sensor conductivity probe and the signal processing scheme, Int. J. Heat Mass Transfer 43 (22) (2000) 4101–4118.
[17] Q. Wu, M. Ishii, Sensitivity study on double-sensor conductivity probe for the measurement of interfacial area concentration in bubbly flow, Int. J. Multiphase Flow 25 (1) (1999) 155–173.